Isogeometric discretizations of the Stokes problem: stability analysis by the macroelement technique.

ANDREA BRESSAN[1,*] AND GIANCARLO SANGALLI[1,2,†]

[1]Dipartimento di Matematica, Università di Pavia,
via Ferrata 1, 27100 Pavia, Italia

[2]IMATI, CNR
via Ferrata 1, 27100 Pavia, Italia

Abstract

We propose and study high-regularity isogeometric discretizations of the Stokes problem. We address the *Taylor-Hood* isogeometric element, already known in this context, and a new *Subgrid* element which allows highest regularity velocity and pressure fields. Our stability analysis grounds on a characterization of full-rank scalar products for splines, which is the key theoretical result of this paper. We include numerical testing on two and three-dimensional benchmarks.

Keywords: Stokes problem, inf sup condition, isogeometric analysis, spline, NURBS.

---

[*] Email: andrea.bressan@unipv.it

[†] Email: giancarlo.sangalli@unipv.it

1 Introduction

This work is devoted to the stability analysis of highly-regular isogeometric elements for the Stokes problem.

Isogeometric analysis has been introduced in 2005 by T.J.R. Hughes and co-authors (see [18]) as a novel technique for the discretization of Partial Differential Equations (PDE). This technique is having a growing impact on several fields, from fluid dynamics [3, 9, 2, 5, 16], to structural mechanics [1, 13, 20] and electromagnetics [11, 10]. A comprehensive reference is the book [12]. Isogeometric methodologies are designed with the aim of a direct interface of the PDE solver to the Computer Aided Design (CAD) system, in order to drastically reduce the error in the representation of the computational domain by the use of the "exact" CAD geometry directly at the coarsest level of discretization. This is achieved adopting B-Splines or Non-Uniform Rational B-Splines (NURBS) functions for the geometry description as well as for the representation of the unknown fields. Splines and NURBS offer a flexible set of basis functions for which mesh refinement (h-refinement) and degree elevation (p-refinement) are very efficient. Beside the fact that in isogeometric analysis one can directly treat geometries described by Splines and NURBS parametrizations, these functions are interesting in themselves since they easily allow global smoothness beyond the classical C^0-continuity of FEM. This feature allows k-refinement, that is, one can refine the space keeping the maximum regularity C^{p-1} when new knots are inserted. Numerical tests shown in literature and the studies [19, 6, 15] proved that higher smoothness is advantageous.

Isogeometric methods for the Stokes problem have been the focus of previous works [4, 7, 9]. The motivation of the present work is to study isogeometric distretizations that extend the Taylor-Hood element, well-known in the finite element context ([25, 8]), to the isogeometric context. These isogeometric Taylor-Hood (*TH*) elements are based on $p+1$ degree NURBS velocity approximation and p degree NURBS pressure approximation. The novelty, in the isogeometric framework, is that C^r global regularity is allowed, up to $r = p-1$. The stability of the isogeometric *TH* element is known from the numerical testing in [4, 9] and has been proved but only for C^0 regularity in [4] and for C^1 regularity in [7]. We cover here the general case.

Our approach is based on an original result about the characterization of the full-rank condition for the L^2-scalar product of spline spaces. It states that given two univariate spline spaces S_1 and S_2, possibly with different degrees and different knot vectors, if $\dim(S_1) \geq \dim(S_2)$, then the scalar product

$$f \in S_1, g \in S_2 \mapsto \int_{\mathbb{R}} f(x)g(x)\,dx$$

is full rank if and only if the degrees-of-freedom density of S_1 is larger or equal to the degrees-of-freedom density of S_2. This is quantified in a rigorous way in Theorem 3.10 and extended to multivariate splines in Theorem 3.13. The full-rank characterization is then used to study the inf sup stability of isogeometric spaces locally, at the *macroelement* level, and then globally, following the macroelement technique [23, 24].

Besides the isogeometric *TH* element, our full-rank characterization indicate that many other isogeometric discretizations of the Stokes problem are stable. Among them, we focus on the interesting case which is referred to as isogeometric subgrid (*SG*) element. This is designed on a velocity mesh which is a subgrid of the pressure mesh, and allows for both velocity and pressure at the highest regularity (typically $(p+1)$-degree C^p-continuous velocities and p-degree C^{p-1}-continuous pressures), in the spirit of k-refinement. Numerical tests show that also in this context the use of discrete fields at highest regularity is beneficial and improves the accuracy versus degrees-of-freedom ratio.

The outline of the paper is as follows. After some preliminaries and notation on splines, NURBS, and isogeometric analysis (Section 2), in Section 3 we present our characterization of the full-rank L^2-scalar product of spline spaces. This result is then used in Section 4 to prove the inf sup stability of the *TH* and *SG* isogeometric elements. Finally, in Section 5 we perform two-dimensional and three-dimensional numerical tests, confirming the stable behaviour of the isogeometric elements mentioned above.

2 Preliminaries

2.1 Spline spaces and notation

This section is devoted to a quick introduction of Spline spaces and to a presentation of the notation we will use. We refer to , e.g., [14, 22], for more details.

Definition 2.1. *Let* p *a non-negative integer and* $\Xi := (\xi_1, \xi_2, \dots, \xi_{n+p+1})$ *a knot vector such that* $\xi_i \le \xi_{i+1}$*. A B-spline space* $S_{p,\Xi}$ *is a space of functions* f *defined on* $\mathbb{R}$*, denoted splines, that satisfy the following conditions (codified in the knot vector)*

1. $f(x) = 0$ *if* $x \notin [\xi_1, \xi_{n+p+1}[$*;*
2. *if* $\xi_i < \xi_{i+1}$ *then* f *is a polynomial of degree at most* p *in* $[\xi_i, \xi_{i+1}[$*;*
3. *let* r *be the maximum integer such that* $\xi_i = \dots = \xi_{i+p-r-1}$ *(with* $-1 \le r \le p-1$*), then* f *has* r *continuous derivatives at* ξ_i*; when* $r = -1$ *a discontinuity (left-jump) is allowed at* ξ_{i+1}*; the quantity* r *is referred as* regularity *at the knot* ξ_i *and* $p - r$ *is referred as* multiplicity *of the knot* ξ_i*.*

Furthermore, we introduce the vector $\mathcal{Z} = (\zeta_1, \dots, \zeta_m)$ of knots *without repetitions*, and the vector $(r_1, \dots, r_m)$ of regularities, such that

$$\Xi = (\underbrace{\zeta_1, \dots, \zeta_1}_{p-r_1 \text{ times}}, \underbrace{\zeta_2, \dots, \zeta_2}_{p-r_2 \text{ times}}, \dots, \underbrace{\zeta_m, \dots, \zeta_m}_{p-r_m \text{ times}}),$$

with $\sum_{i=1}^{m}(p - r_i) = n + p + 1$. The vector $\mathcal{Z}$ induces a *partition* of $[\zeta_1, \zeta_m[$ into elements $[\zeta_i, \zeta_{i+1}[$. A knot vector is said to be *open* when $p - r_1 = p - r_m = p + 1$.

Remark 2.2. By definition, all spline functions in $S_{p,\Xi}$, and their derivatives, are right-continuous everywhere, and C^∞ in $\mathbb{R} \setminus \{\zeta_1, \dots, \zeta_m\}$.

The dimension of the spline space $S_{p,\Xi}$ is

$$\dim S_{p,\Xi} = (p+1)(m-1) - \sum_{i=1}^{m}(r_1 + 1) = n. \tag{1}$$

The spline space $S_{p,\Xi}$ has a canonical basis $\{B_i\}$ defined recursively over p by

$$B_{i,0}(x) = \begin{cases} 1 & x \in [\xi_i, \xi_{i+1}[, \\ 0 & \text{otherwise}, \end{cases} \tag{2}$$

$$B_{i,k}(x) = \frac{x - \xi_i}{\xi_{i+k} - \xi_i} B_{i,k-1}(x) - \frac{x - \xi_{i+k+1}}{\xi_{i+k+1} - \xi_{i+1}} B_{i+1,k-1}(x), \tag{3}$$

$$B_i = B_{i,p}, \tag{4}$$

where, in (3), we assume $0/0 = 0$. This basis has some noteworthy properties:

1. $\forall i = 1, 2, \dots, n$, $\forall x \in \mathbb{R}$, $B_i(x) \ge 0$;
2. B_i is non-null in $[\xi_i, \xi_{i+p+1}[$, then $\operatorname{supp} B_i = \overline{\{x \in \mathbb{R} : B_i(x) \ne 0\}} = [\xi_i, \xi_{i+p+1}]$, where $\overline{J}$ is the closure of J;
3. the basis $\{B_i\}$ is a partition of unity of the interval $[\xi_{p+1}, \xi_{n+1}[$, that is, $\sum_{i=1}^{n} B_i(x) = 1$ for all $x \in [\xi_p, \xi_{n+1}[$.

In some situations, spline spaces are considered as defined over the closed interval $[\zeta_1, \zeta_m]$. In this case the space $S_{p,\Xi}$ contains the restrictions of the functions as defined above to $[\zeta_1, \zeta_m[$ and extended by continuity in ζ_m. However, for the results we shall present in Section 3, it is more convenient to assume that splines are defined on $\mathbb{R}$, which is our choice.

Remark 2.3. In our examples we will often restrict, for the sake of simplicity, to the case where the smoothness at the knots is constant. If $r = r_2 = \ldots = r_{m-1}$ and the knot vector is open ($r_1 = r_m = -1$), the spline space will be denoted by $S_{p,r,\mathcal{Z}}$. If $r = r_1 = r_2 = \ldots = r_m$ then we will use the notation $\mathring{S}_{p,r,\mathcal{Z}}$.

Remark 2.4. Let $p \geq 1$ and $S_{p,\Xi} \subset C^0(\mathbb{R})$, we define

$$\partial S_{p,\Xi} = \left\{ \frac{\partial}{\partial x} f \, : \, f \in S_{p,\Xi} \right\}. \tag{5}$$

Derivatives of continuous splines are splines, of lower degree and regularity. When $\Xi = (\xi_1, \xi_2, \ldots, \xi_{n+p+1})$ is an open knot vector we have in particular $\partial S_{p,\Xi} = S_{p-1,\Xi'}$, where $\Xi' = (\xi_2, \xi_3, \ldots, \xi_{n+p})$, that is, we obtain Ξ' from Ξ removing the first and last knots.

Multivariate B-splines in d-dimensions are obtained by tensor-product multiplication of uni-variate splines in each variable, thus a multivariate spline space is defined in terms of a vector of degrees $\boldsymbol{p} = (p_1, \ldots, p_d)$ and a vector of knot vectors $\boldsymbol{\Xi} = (\Xi_1, \ldots, \Xi_d)$:

$$S_{\boldsymbol{p},\boldsymbol{\Xi}} = S_{p_1,\Xi_1} \otimes \cdots \otimes S_{p_d,\Xi_d}. \tag{6}$$

In this case, the canonical basis is

$$B_{\boldsymbol{i}}(x_1, \ldots, x_d) = B_{1,i_1}(x_1) \ldots B_{d,i_d}(x_d), \tag{7}$$

where $\boldsymbol{i} = (i_1, \ldots, i_d)$ and $\{B_{j,i}\}_{i=1,\ldots,n_j}$ is the canonical basis of S_{p_j,Ξ_j}. To $\boldsymbol{\Xi}$ correspond the vector of knot vector without repetitions $\boldsymbol{\mathcal{Z}} = (\mathcal{Z}_1, \ldots, \mathcal{Z}_d)$ with $\mathcal{Z}_j = (\zeta_{j,1}, \ldots, \zeta_{j,m_j})$. Therefore on the so-called *parametric domain*

$$\widehat{\Omega} = [\zeta_{1,1}, \zeta_{1,m_1}[\times \ldots \times [\zeta_{d,1}, \zeta_{d,m_d}[\tag{8}$$

it is defined a partition

$$\widehat{\mathscr{T}_{\boldsymbol{\mathcal{Z}}}} = \left\{ [\zeta_{1,j_1}, \zeta_{1,j_1+1}[\times \ldots \times [\zeta_{d,j_d}, \zeta_{d,j_d+1}[\right\}_{\substack{i=1,\ldots,d,\\ j_i=1,\ldots,m_i-1.}} \tag{9}$$

The support of all splines of $S_{\boldsymbol{p},\boldsymbol{\Xi}}$ is included in the closure of $\widehat{\Omega}$. As in the one-dimensional case, we use the notation $S_{p,r,\boldsymbol{\mathcal{Z}}}$ to denote $S_{\boldsymbol{p},\boldsymbol{\Xi}}$ if the degree is p and the regularity at the internal knots is r in all tensor-product components and $\mathring{S}_{p,r,\boldsymbol{\mathcal{Z}}}$ if the regularity is r at all the knots.

2.2 NURBS and isogeometric analysis

A very short description of NURBS spaces and NURBS maps is given in this section. More on isogeometric analysis can be found in [18, 12]

Non Uniform Rational B-Splines functions are quotients of spline functions. A NURBS space is described by a spline space $S_{\boldsymbol{p},\boldsymbol{\Xi}}$ and a strictly positive *weight function* $\omega \in S_{\boldsymbol{p},\boldsymbol{\Xi}}$:

$$N_{\boldsymbol{p},\boldsymbol{\Xi}} = \left\{ \frac{f}{\omega} : f \in S_{\boldsymbol{p},\boldsymbol{\Xi}} \right\}; \tag{10}$$

the weight ω is not shown in the notation because in this context it is assumed to be given as a datum of the problem, and is not changed during mesh refinement or degree elevation. As above, $N_{p,r,\boldsymbol{\mathcal{Z}}}$ denotes the special case of a NURBS space of degree p in all tensor-product components, on the mesh $\widehat{\mathscr{T}_{\boldsymbol{\mathcal{Z}}}}$ having internal knots of multiplicity $p - r$; the global regularity of $N_{p,r,\boldsymbol{\mathcal{Z}}}$ is then C^r.

NURBS functions are a fundamental tool in computer graphics, see for example [21]. In the isogeometric method the *physical domain* of interest Ω is given as the image of the parametric domain $\widehat{\Omega}$ through a continuous map $F : \widehat{\Omega} \to \mathbb{R}^d$ whose components are in a NURBS space $N_{p_0,r_0,\boldsymbol{\mathcal{Z}}_0}$ and thus share the same weight denominator ω. In this context, F and ω are considered data of the problem. Typically, F is given at a coarse level of discretization, while refined NURBS spaces are used for the discretization of unknown fields. Then, if Φ be is a space of scalar fields on Ω, its isogeometric discretization is obtained invoking the *isoparametric* approach, that is, one considers the space

$$\Phi_{p,\boldsymbol{\Xi}} = \{f \circ F^{-1} : f \in N_{p,\boldsymbol{\Xi}}\}, \tag{11}$$

where $N_{p,\boldsymbol{\Xi}}$ is a NURBS space that refines $N_{p_0,r_0,\boldsymbol{\mathcal{Z}_0}}$. Discretization of vector fields is analogous: each component is discretized as (11). The mesh $\mathscr{T}_{\boldsymbol{\mathcal{Z}}}$ on Ω is defined by the image of the mesh $\widehat{\mathscr{T}_{\boldsymbol{\mathcal{Z}}}}$ in the parametric space:

$$\mathscr{T}_{\boldsymbol{\mathcal{Z}}} = \left\{K = F(\widehat{K}) : \widehat{K} \in \widehat{\mathscr{T}_{\boldsymbol{\mathcal{Z}}}}\right\}. \tag{12}$$

As usual in finite elements analysis, the vector of knot vectors $\boldsymbol{\mathcal{Z}}$ is sometimes replaced by the family index h that refers to the mesh size. The meanings of the symbols $\mathscr{T}_h$ and $N_{p,r,h}$ are respectively $\mathscr{T}_{\boldsymbol{\mathcal{Z}}}$ and $N_{p,r,\boldsymbol{\mathcal{Z}}}$ where $\boldsymbol{\mathcal{Z}}$ is such that

$$\max\{\operatorname{diam}(K) : K \in \mathscr{T}_{\boldsymbol{\mathcal{Z}}}\} \leq h.$$

Note that, by convention, when two symbols contains the same family index h then they are defined on the same partition $\mathcal{Z}$. An addition assumption in isogeometric analysis is that all meshes $\mathscr{T}_h$ are refinements of the coarse mesh $\mathscr{T}_{\boldsymbol{\mathcal{Z}}_0} = \mathscr{T}_{h_0}$.

3 Rank of L^2-scalar product between spline spaces

3.1 Zeros and sign changes

We recall some definitions from [14].

Definition 3.1 (Sign change)**.** *A function f changes sign across x (equivalently, x is a sign change of f) if $\forall \epsilon > 0$ there exists $x^- \in]x-\epsilon, x[$ and $x^+ \in]x, x+\epsilon[$ such that $f(x^-)f(x^+) < 0$.*

Definition 3.2 (Zero)**.** *A zero of a function f is a maximal closed interval z such that its interior is a subset of $f^{-1}(0)$. The set of all zeros of f is denoted by $\mathcal{Z}(f)$.*

Definition 3.3 (Zero multiplicity)**.** *Let $S_{p,\Xi}$ be a given spline space and $f \in S_{p,\Xi}$. The multiplicity $z^{\#}$ of a zero $z \in \mathcal{Z}(f)$ is the maximum integer α such that for all open interval $J \supset z$ and for all L^∞-neighborhood $\mathcal{H}$ of f there exists a $g \in \mathcal{H} \cap S_{p,\Xi}$ that admits α sign changes in J.*

According to the previous Definition 3.2, every x in the domain of f belongs to a zero of f, that is, either x belongs to an *interval zero* $[a, b]$ such that $a < b$, or $\{x\}$ is an *isolated* zero of f. This unusual definition of zero is complemented by the notion of of Definition 3.3. Notice that $z^{\#}$ depends on f *and* on the ambient space $S_{p,\Xi}$ which is taken into consideration, not appearing in the notation.

Remark 3.4. With an abuse of notation, in the following we will refer to z as a zero only when $z^{\#} \geq 1$.

Remark 3.5. We have the following one to one correspondence (see [14, Section 4]): x is a sign change of f if and only if $\{x\}$ is a zero of odd order

Definition 3.6. *Let $f \in S_{p,\Xi}$. The zero count of f relative to $S_{p,\Xi}$ is*

$$\mathcal{Z}^{\#}(f) = \sum_{z \in \mathcal{Z}(f)} z^{\#}. \tag{13}$$

The zero count $\mathcal{Z}^{\#}(f)$ is bounded by the number of sign changes in the coefficients of f with respect to the canonical basis (2)–(4) (see [14, 17]). Thus, in general, we have the following result.

Corollary 3.7. *For all $f \in S_{p,\Xi}$ it holds*

$$\mathcal{Z}^{\#}(f) \leq \dim S_{p,\Xi} - 1. \tag{14}$$

In the next section we will also need the following corollary.

Corollary 3.8. *Given $f \in S_{p,\Xi}$, there exist $x_0, \ldots, x_k$ with $\xi_1 = x_0 < x_1 < \ldots < x_{k-1} < x_k = \xi_{n+p+1}$ and $k \leq n = \dim S_{p,\Xi}$, and there exists $C = \pm 1$ such that for all $i = 1, \ldots, k$*

$$C(-1)^i f|_{[x_{i-1},x_i[} \geq 0. \tag{15}$$

Proof. Set $C = 1$ and assume that $f(x) \leq 0$ in a right neighborhood of $\xi_1 = x_0$. If this is not the case, replace f with $-f$ in what follows, and set $C = -1$.

We define $x_1, x_2, \ldots, x_k$ as

$$x_i = \sup \left\{ x \in]x_{i-1}, \xi_{n+p+1}] \, : \, (-1)^i f|_{[x_{i-1},x[} \geq 0 \right\}. \tag{16}$$

Observe that for the assumption above, x_1 is well defined. Let now $i > 2$. Assuming that x_{i-1} is defined, and $x_{i-1} < \xi_{n+p+1}$, (16) and the right-continuity of f (see Remark 2.2) imply that

$$(-1)^i f|_{]x_{i-1},x_{i-1}+\varepsilon[} > 0, \tag{17}$$

for some $\varepsilon > 0$. Then the set $\left\{ x \in]x_{i-1}, \xi_{n+p+1}] \, : \, (-1)^i f|_{[x_{i-1},x[} \geq 0 \right\}$ is non-empty and (16) defines x_i.

This construction terminates after finite recursion steps with $x_k = \xi_{n+p+1}$. Indeed, each x_i, $i = 1, \ldots, k-1$, belongs to $]\xi_1, \xi_{n+p+1}[$ and is, from definition, either the right endpoint of an interval zero (if $f|_{]x_i-\epsilon,x_i[} = 0$, for some $\epsilon > 0$) or $\{x_i\}$ is an isolated zero (when $(-1)^{i+1} f|_{]x_i-\epsilon,x_i[} > 0$, for some $\epsilon > 0$). Using (14), we have $k - 1 \leq \dim S_{p,\Xi} - 1$.

□

3.2 L^2-scalar product of splines in one-dimension

We first introduce a notation for restrictions of spline spaces.

Definition 3.9. *Let $\Xi := (\xi_1, \xi_2, \ldots, \xi_{n+p+1})$ be a given knot vector, $S = S_{p,\Xi}$ the associated spline space and $J = [a, b[$ such that $\xi_1 \leq a < b \leq \xi_{n+p+1}$. We define*

$$S_{\subset J} = \operatorname{span}\{B_i \in S : \; B_i(x) = 0, \, \forall x \in \mathbb{R} \backslash J\}, \tag{18}$$

$$S_{\cap J} = \operatorname{span}\{B_i \in S : B_i|_J \neq 0\}, \tag{19}$$

where $\{B_i\}$ is the canonical basis of S.

It is easily seen that both $S_{\subset J}$ and $S_{\cap J}$ are spline spaces, subspaces of S. Indeed,

$$S_{\subset J} = S_{p,(\xi_i,\xi_{i+1},\ldots,\xi_j)},$$

where $\xi_{i-1} < a \leq \xi_i$ and $\xi_j \leq b < \xi_{j+1}$, while

$$S_{\cap J} = S_{p,(\xi_{i-p-1},\xi_{i-p},\ldots,\xi_{j+p+1})},$$

where, now, $\xi_{i-1} \leq a < \xi_i$ and $\xi_j < b \leq \xi_{j+1}$ (in the previous inequalities, $\xi_{-1} = -\infty$ and $\xi_{n+p+2} = +\infty$).

Consider now two spline spaces $S_1 = S_{p_1,\Xi_1}$ and $S_2 = S_{p_2,\Xi_2}$ with $\Xi_1 := (\xi_{1,1}, \xi_{1,2}, \dots, \xi_{1,n_1+p_1+1})$, $\Xi_2 := (\xi_{2,1}, \xi_{2,2}, \dots, \xi_{2,n_2+p_2+1})$. Let $\mathcal{Z}_1 = (\zeta_{1,1}, \dots, \zeta_{1,m_1})$ be the knot vectors without repetitions corresponding to Ξ_1. We want to study the L^2-scalar product

$$f, g \mapsto \int_{\mathbb{R}} f(x)g(x)\,dx \tag{20}$$

which is well defined on $S_1 \times S_2$. In particular we want to characterize when the rank of (20) is equal to $\dim S_2 = n_2$. This is equivalent to the property that

$$\text{the matrix } \left(\int_{\mathbb{R}} B_{1,i}(x)B_{2,j}(x)\,dx\right)_{\substack{i=1,\dots,n_1\\ j=1,\dots,n_2}} \text{ has full rank and } n_1 \geq n_2, \tag{21}$$

where $\{B_{1,i}(x)\}_{i=1,\dots,n_1}$ and $\{B_{2,j}(x)\}_{j=1,\dots,n_2}$ are the canonical basis of S_1 and S_2, respectively. A less straightforward, but more useful characterization is given in the next theorem, which is the key tool for the next sections.

Theorem 3.10. *Assuming that*

$$[\zeta_{2,1}, \zeta_{2,m_2}] \subseteq [\zeta_{1,1}, \zeta_{1,m_1}] \tag{22}$$

the following two properties are equivalent:

$$\textit{for all } 1 \leq i < j \leq m_1,\ \dim S_{1\cap[\zeta_{1,i},\zeta_{1,j}[} \geq \dim S_{2\subset[\zeta_{1,i},\zeta_{1,j}[};\tag{23}$$

$$\textit{for all } g \in S_2,\ g \neq 0,\ \textit{there exists } f \in S_1 \textit{ such that } \int_{\mathbb{R}} f(x)g(x)\,dx \neq 0. \tag{24}$$

Proof. We begin by proving the implication (23)⇒(24). Then, let us assume (23), which by (22) implies

$$\dim S_1 \geq \dim S_2 \tag{25}$$

and let $0 \neq g \in S_2$. We also assume, for the moment, that

$$\text{for all non-null } f \in S_1, \quad |\operatorname{supp} f \cap \operatorname{supp} g| > 0, \tag{26}$$

where $|J|$ is the measure of J.

Thanks to Corollary 3.8 applied to g we get $x_0, \dots, x_k$, with

$$k \leq n_2 = \dim S_2 \tag{27}$$

such that

$$\forall i = 1, \dots, k, \quad C(-1)^i g|_{[x_{i-1}, x_i[} \geq 0. \tag{28}$$

Given indexes s, t such that $1 \leq s < t \leq n_1 + p_1 + 1$, consider the knot vector $(\xi_{1,s}, \dots, \xi_{1,t})$, its related space $S_{p_1,(\xi_{1,s},\dots,\xi_{1,t})} \subset S_1$, and the subspace

$$S^{\sim}_{p_1,(\xi_{1,s},\dots,\xi_{1,t})} = \left\{v \in S_{p_1,(\xi_{1,s},\dots,\xi_{1,t})} : \forall i = 1, \dots, k-1,\ v(x_i) = 0\right\}. \tag{29}$$

Observe that in (29) each zero condition $v(x_i) = 0$ acts as a linear constraint; moreover, from (27) and (25), the total number of such constraints (not necessarily independent) is $k - 1 \leq \dim S_1 - 1$. This gives

$$\dim S^{\sim}_{p_1,(\xi_{1,0},\dots,\xi_{1,n_1+p_1+1})} \geq \dim S_1 - (k-1) \geq 1.$$

We also have

$$\dim S^{\sim}_{p_1,(\xi_{1,s},\dots,\xi_{1,s+p_1+1})} \leq \dim S_{p_1,(\xi_{1,s},\dots,\xi_{1,s+p_1+1})} = 1.$$

Moreover, by reducing by one knot the knot vector $(\xi_{1,s}, \dots, \xi_{1,t})$ either the dimension of $S^{\sim}_{p_1,(\xi_{1,s},\dots,\xi_{1,t})}$ decreases by one or is preserved, that is

$$\dim S^{\sim}_{p_1,(\xi_{1,s},\dots,\xi_{1,t})} - 1 \leq \dim S^{\sim}_{p_1,(\xi_{1,s},\dots,\xi_{1,t-1})} \leq \dim S^{\sim}_{p_1,(\xi_{1,s},\dots,\xi_{1,t})},$$

$$\dim S^{\sim}_{p_1,(\xi_{1,s},\dots,\xi_{1,t})} - 1 \leq \dim S^{\sim}_{p_1,(\xi_{1,s+1},\dots,\xi_{1,t})} \leq \dim S^{\sim}_{p_1,(\xi_{1,s},\dots,\xi_{1,t})}.$$

Therefore we can then select s, t such that

$$\dim S^{\sim}_{p_1,(\xi_{1,s},\dots,\xi_{1,t})} = 1 \tag{30}$$

and

$$t - s \text{ is minimal.} \tag{31}$$

From now on, s and t are selected in order to fulfill (30)–(31). We have the following property:

$$\text{if } v \in S_{p_1,(\xi_{1,s},\dots,\xi_{1,t})} \text{ and } x_i \notin]\xi_{1,s}, \xi_{1,t}[\text{ then } v(x_i) = 0. \tag{32}$$

Indeed, all functions in $S_{p_1,(\xi_{1,s},\dots,\xi_{1,t})}$ vanish on $\mathbb{R} \setminus [\xi_{1,s}, \xi_{1,t}[$, since Definition 2.1. Furthermore, if $x_i = \xi_{1,s}$ (for some i) then the minimality condition (31) implies $\xi_{1,s} < \xi_{1,s+p_1}$, giving $v(x_i) = 0$ for all $v \in S_{p_1,(\xi_{1,s},\dots,\xi_{1,t})}$ (again from Definition 2.1). Indeed, if $\xi_{1,s} = \xi_{1,s+p_1}$ then $S^{\sim}_{p_1,(\xi_{1,s},\dots,\xi_{1,t})} = S^{\sim}_{p_1,(\xi_{1,s+1},\dots,\xi_{1,t})}$. Using (32) we can write

$$S^{\sim}_{p_1,(\xi_{1,s},\dots,\xi_{1,t})} = \left\{ v \in S_{p_1,(\xi_{1,s},\dots,\xi_{1,t})} : \forall x_i \in]\xi_{1,s}, \xi_{1,t}[,\ v(x_i) = 0 \right\},$$

and so

$$\begin{aligned} \#\{x_i : x_i \in]\xi_{1,s}, \xi_{1,t}[\} &\geq \dim S_{p_1,(\xi_{1,s},\dots,\xi_{1,t})} - \dim S^{\sim}_{p_1,(\xi_{1,s},\dots,\xi_{1,t})} \\ &= \dim S_{p_1,(\xi_{1,s},\dots,\xi_{1,t})} - 1. \end{aligned} \tag{33}$$

Let $f \in S_{p_1,(\xi_{1,s},\dots,\xi_{1,t})}$ such that $S^{\sim}_{p_1,(\xi_{1,s},\dots,\xi_{1,t})} = \operatorname{span}\{f\}$. From (30), $\operatorname{supp} f$ has to be an interval, and from (31) it has to be the whole $[\xi_{1,s}, \xi_{1,t}]$. This means that all (non null multiplicity) zeros $z \subset (\xi_{1,s}, \xi_{1,t})$ of $f \in S_{p_1,(\xi_{1,s},\dots,\xi_{1,t})}$ are isolated zeros. Then we know that $z = \{x_i\}$, for all $x_i \in]\xi_{1,s}, \xi_{1,t}[$ are (non null multiplicity) zeros of f. Because of Corollary 3.7 and (33), they are all the zeros of f and that their multiplicity is 1. Thus they are the sign changes (see Remark 3.5) and

$$\forall i = 1, \dots, k, \quad C(-1)^i f|_{[x_{i-1}, x_i[} \geq 0. \tag{34}$$

Under assumption (26), recalling (28) and (34), we have $\int_{\mathbb{R}} f(x) g(x)\, dx \neq 0$ and (24) is proved.

It remains to deal with the case when (26) does not hold. In that case the set

$$U = \bigcup_{f \in S_1 : |\operatorname{supp} f \cap \operatorname{supp} g| = 0} \operatorname{supp} f, \tag{35}$$

in non-empty. From its definition, U is the union of intervals of the form $[\zeta_{1,i}, \zeta_{1,j}]$. Select a maximal interval $[\zeta_{1,s}, \zeta_{1,t}]$ such that $]\zeta_{1,s}, \zeta_{1,t}[\subset \mathbb{R} \setminus U$. Then $\operatorname{supp} g$ has a connected component which is contained in $[\zeta_{1,s}, \zeta_{1,t}]$. Precisely, from the definition above, if $s > 1$ then there is a basis function in S_1 with support $[\zeta_{1,s^-}, \zeta_{1,s}]$ such that

$$g \text{ is null on } [\zeta_{1,s^-}, \zeta_{1,s}[. \tag{36}$$

Analogously if $t < m_1$ there is a basis function in S_1 supported in $[\zeta_{1,t}, \zeta_{1,t^+}]$ such that

$$g \text{ is null on } [\zeta_{1,t}, \zeta_{1,t^+}[. \tag{37}$$

Define

$$\tilde{g}(x) = \begin{cases} g(x), & \text{if } x \in [\zeta_{1,s}, \zeta_{1,t}[, \\ 0, & \text{if } x \in \mathbb{R} \setminus [\zeta_{1,s}, \zeta_{1,t}[. \end{cases}$$

Since (36)–(37), $\tilde{g}(x) \in S_{2\subset[\zeta_{1,s},\zeta_{1,t}[}$. We can now replace S_1 by $S_{1\cap[\zeta_{1,s},\zeta_{1,t}[}$ and S_2 by $S_{2\subset[\zeta_{1,s},\zeta_{1,t}[}$: then hypothesis (23) and equation (26) hold. Thus, as we have proved above, there exists $f \in S_{1\cap[\zeta_{1,s},\zeta_{1,t}[}$ such that $\int_{\mathbb{R}} f(x)\tilde{g}(x)\,dx \neq 0$. However, still from (36)–(37), for all $f \in S_{1\cap[\zeta_{1,s},\zeta_{1,t}[}$ we have

$$\int_{\mathbb{R}} f(x)g(x)\,dx = \int_{\mathbb{R}} f(x)\tilde{g}(x)\,dx,$$

and (24) follows.

Finally, we prove the implication (24)⇒(23). Assume (23) does not hold. Then $\dim S_{1\cap[\zeta_{1,i},\zeta_{1,j}[} < \dim S_{2\subset[\zeta_{1,i},\zeta_{1,j}[}$ for some $[\zeta_{1,i},\zeta_{1,j}[$, and thus there exists a non-null $g \in S_{2\subset[\zeta_{1,i},\zeta_{1,j}[}$ which is L^2-orthogonal to $S_{1\cap[\zeta_{1,i},\zeta_{1,j}[}$. Since, by definition, $g = 0$ in $\mathbb{R}\backslash[\zeta_{1,i},\zeta_{1,j}[$ and

$$\{v|_{[\zeta_{1,i},\zeta_{1,j}[} : v \in S_{1\cap[\zeta_{1,i},\zeta_{1,j}[}\} = \{v|_{[\zeta_{1,i},\zeta_{1,j}[} : v \in S_1\},$$

for all $f \in S_1$ we have

$$\int_{\mathbb{R}} f(x)g(x)\,dx = \int_{\mathbb{R}\backslash[\zeta_{1,i},\zeta_{1,j}[} f(x)g(x)\,dx + \int_{[\zeta_{1,i},\zeta_{1,j}[} f(x)g(x)\,dx = 0, \tag{38}$$

that is, (24) fails. □

The following statements focus on condition (23) for two special cases involving spaces of uniform regularity (recall Remark 2.3). These results will be used in Section 4.3.

Proposition 3.11. *Let* $S_1 = \mathring{S}_{p_1,r_1,\mathcal{Z}}$ *and* $S_2 = S_{p_2,r_2,\mathcal{Z}}$ *be associated to the same partition* $\mathcal{Z} = (\zeta_1,\ldots,\zeta_m)$*. Sufficient conditions for* (23) *are*

1. $\dim S_1 \geq \dim S_2$;
2. $p_1 - r_1 \geq p_2 - r_2$.

Proof. Observe that $\dim S_{1\cap[\zeta_i,\zeta_{i+1}[}$ is $p_1 + 1$ for elements $[\zeta_i,\zeta_{i+1}[$ that are far enough from the endpoints ζ_1 and ζ_m. Precisely, when both i and $m - i$ are $\geq \lceil (p_1+1)/(p_1-r_1) \rceil$. Otherwise $\dim S_{1\cap[\zeta_i,\zeta_{i+1}[}$ is less than $p_1 + 1$. In order to prove (23) we consider the following cases:

1. if $\dim S_{1\cap[\zeta_s,\zeta_{s+1}[} < p_1 + 1$, $\dim S_{1\cap[\zeta_{t-1},\zeta_t[} < p_1 + 1$ then $S_{1\cap[\zeta_s,\zeta_{s+1}[} = S_1$ and

   $$\dim S_{1\cap[\zeta_s,\zeta_t[} = \dim S_1 \geq \dim S_2 \geq \dim S_{2\subset[\zeta_s,\zeta_t[},$$

   from hypotesis 1;

2. if $\dim S_{1\cap[\zeta_s,\zeta_{s+1}[} = \dim S_{1\cap[\zeta_{t-1},\zeta_t[} = p_1 + 1$ then

   $$\begin{aligned}\dim S_{1\cap[\zeta_s,\zeta_t[} &= p_1 + 1 + (p_1 - r_1)(t - s - 1)\\ &\geq p_2 - r_2 + (p_2 - r_2)(t - s - 1) \geq S_{2\subset[\zeta_s,\zeta_t[};\end{aligned}$$

3. if $\dim S_{1\cap[\zeta_s,\zeta_{s+1}[} = p_1 + 1$, $\dim S_{1\cap[\zeta_{t-1},\zeta_t[} < p_1 + 1$ then

   $$\begin{aligned}\dim S_{1\cap[\zeta_s,\zeta_t[} &= (p_1 - r_1)(m - s)\\ &\geq (p_2 - r_2)(m - s) \geq S_{2\subset[\zeta_s,\zeta_t[};\end{aligned}$$

4. if $\dim S_{1\cap[\zeta_s,\zeta_{s+1}[} < p_1 + 1$, $\dim S_{1\cap[\zeta_{t-1},\zeta_t[} = p_1 + 1$ then this case is specular to the previous one.

□

Another interesting case is when the partition $\mathcal{Z}_1$ corresponding to S_1 is a *refinement* of the partition $\mathcal{Z}_2$ corresponding to S_2. In particular given $\mathcal{Z}_2 = (\zeta_{2,1}, \dots, \zeta_{2,m_2})$ consider $\mathcal{Z}_1 = (\zeta_{1,1}, \dots, \zeta_{1,m_1})$, $m_1 = 2m_2 - 1$, defined by

$$\mathcal{Z}_1 = \left(\zeta_{2,1}, \frac{\zeta_{2,1} + \zeta_{2,2}}{2}, \zeta_{2,2}, \dots\dots, \frac{\zeta_{2,m_2-1} + \zeta_{2,m_2}}{2}, \zeta_{2,m_2}\right). \tag{39}$$

Proposition 3.12. *Given $\mathcal{Z}_1$ and $\mathcal{Z}_2$ as above, let $S_1 = \mathring{S}_{p_1,r_1,\mathcal{Z}_1}$ and $S_2 = S_{p_2,r_2,\mathcal{Z}_2}$. Sufficient conditions for* (23) *are*

1. $\dim S_1 \geq \dim S_2$;
2. $2(p_1 - r_1) \geq p_2 - r_2$.

Proof. We reason as in the proof of Proposition 3.11 and consider the cases:

1. if $\dim S_{1 \cap [\zeta_{1,s}, \zeta_{1,s+1}[} < p_1 + 1$, $\dim S_{1 \cap [\zeta_{1,t-1}, \zeta_{1,t}[} < p_1 + 1$ then $S_{1 \cap [\zeta_{1,s}, \zeta_{1,s+1}[} = S_1$ and
$$\dim S_{1 \cap [\zeta_{1,s}, \zeta_{1,t}[} = \dim S_1 \geq \dim S_2 \geq \dim S_{2 \subset [\zeta_{1,s}, \zeta_{1,t}[},$$
from hypothesis 1;
2. if $\dim S_{1 \cap [\zeta_{1,s}, \zeta_{1,s+1}[} = \dim S_{1 \cap [\zeta_{1,t-1}, \zeta_{1,t}[} = p_1 + 1$ then
$$\begin{aligned} \dim S_{1 \cap [\zeta_{1,s}, \zeta_{1,t}[} &= p_1 + 1 + (p_1 - r_1)(t - s - 1) \\ &\geq p_2 - r_2 + (p_2 - r_2) \left\lfloor \frac{t-s-1}{2} \right\rfloor \geq S_{2 \subset [\zeta_{1,s}, \zeta_{1,t}[}; \end{aligned}$$
3. if $\dim S_{1 \cap [\zeta_{1,s}, \zeta_{1,s+1}[} = p_1 + 1$, $\dim S_{1 \cap [\zeta_{1,t-1}, \zeta_{1,t}[} < p_1 + 1$ then
$$\begin{aligned} \dim S_{1 \cap [\zeta_{1,s}, \zeta_{1,t}[} &= (p_1 - r_1)(m - s) \\ &\geq (p_2 - r_2) \left\lfloor \frac{m-s}{2} \right\rfloor \geq S_{2 \subset [\zeta_{1,s}, \zeta_{1,t}[}; \end{aligned}$$
4. if $\dim S_{1 \cap [\zeta_{1,s}, \zeta_{1,s+1}[} < p_1 + 1$, $\dim S_{1 \cap [\zeta_{1,t-1}, \zeta_{1,t}[} = p_1 + 1$ then this case is specular to the previous one.

□

Using the same approach of Proposition 3.12, it is possible to show criteria for partitions of any meshsize ratio. In particular if $\mathcal{Z}_1$, $\mathcal{Z}_2$ are refinements of a common $\mathcal{Z}_0$ respectively obtained by dividing each element in k_1, k_2 uniform elements then the hypothesis 2 would be $k_1(p_1 - r_1) \geq k_2(p_2 - r_2)$.

3.3 L^2-scalar product of splines in d-dimensions

Thanks to the tensor-product structure, the multi-dimensional cases of interest can be easily reduced to the one-dimensional case addressed in Theorem 3.10.

Theorem 3.13. *Given the two d-dimensional tensor-product spline spaces $S_1 = S_{\boldsymbol{p}_1, \boldsymbol{\Xi}_1} = S_{p_{1,1},\Xi_{1,1}} \otimes \cdots \otimes S_{p_{1,d},\Xi_{1,d}}$ and $S_2 = S_{\boldsymbol{p}_2, \boldsymbol{\Xi}_2} = S_{p_{2,1},\Xi_{2,1}} \otimes \cdots \otimes S_{p_{2,d},\Xi_{2,d}}$ such that*

$$\forall i = 1, \dots, d,\ \forall S_{p_{1,i},\Xi_{1,i}} \text{ and } S_{p_{2,i},\Xi_{2,i}} \text{ condition (22) holds,} \tag{40}$$

then, the following propositions are equivalent

$$\forall i = 1, \dots, d,\ \text{(23) holds for the spaces } S_{p_{1,i},\Xi_{1,i}} \text{ and } S_{p_{2,i},\Xi_{2,i}}, \tag{41}$$

$$\forall g \in S_2,\ g \neq 0,\ \exists f \in S_1 \text{ such that } \int_{\mathbb{R}^d} f(\boldsymbol{x}) g(\boldsymbol{x})\, d\boldsymbol{x} \neq 0. \tag{42}$$

Proof. All functions $g \in S_2$ admit a decomposition of the form

$$g(\boldsymbol{x}) = \sum_{\boldsymbol{i}} \beta_{\boldsymbol{i}} B_{\boldsymbol{i}}(\boldsymbol{x}) = \sum_{\boldsymbol{i}} \beta_{\boldsymbol{i}} \prod_{j=1}^{d} B_{j,i_j}(x_j), \tag{43}$$

where $\{B_{j,i}\}$ is the canonical basis of $S_{p_{2,j},\Xi_{2,j}}$.

It is easy to see that (41) implies (42). Indeed, by Theorem 3.10, and recalling the equivalence between (21) and (24), $\forall j = 1, \dots, d$ there exist functions $B^{*}_{j,i} \in S_{p_{1,i},\Xi_{1,i}}$ such that $\forall i, k = 0, \dots, \dim S_{p_{2,i},\Xi_{2,i}}$ $\langle B^{*}_{j,i},\, B_{j,k}\rangle = \delta_{i,\,k}$. Let $0 \neq g \in S_2$ as in (43), then setting

$$f = \sum_{\boldsymbol{i}} \beta_{\boldsymbol{i}} \prod_{j=1}^{d} B^{j,*}_{i_j}(x_j), \tag{44}$$

and applying the Fubini-Tonelli theorem gives

$$\int_{\mathbb{R}^d} g(\boldsymbol{x}) f(\boldsymbol{x}) d\boldsymbol{x} = \sum_{\boldsymbol{i}} \beta_{\boldsymbol{i}}^2 > 0. \tag{45}$$

We have now to prove that (42) implies (41). Assume (41) does not hold. Therefore, by Theorem 3.10, for some k there exist a non-null $\tilde{q}_k \in S_{p_{2,k},\Xi_{2,k}}$ such that $\forall f_k \in S_{p_{1,k},\Xi_{1,k}}$, $\int_{\mathbb{R}} \tilde{q}_k(x_k) f_k(x_k)\, dx_k = 0$. Then for all choices of $0 \neq q_i(x_i) \in S_{p_{2,i},\Xi_{2,i}}$ $i = 1, \dots, k-1, k+1, \dots, d$, the function $q(\boldsymbol{x}) = \prod_{i=1}^{d} q_i(x_i)$ is in S_2. Using the Fubini-Tonelli theorem again, it follows that for all $f \in S_1$

$$\int_{\mathbb{R}^d} q(\boldsymbol{x}) f(\boldsymbol{x}) d\boldsymbol{x} = 0. \tag{46}$$

□

The following corollary concerns a full-rank condition that involves derivatives. It will be used for the stability analysis of the Stokes problem. Recall the notation of (5).

Corollary 3.14. *Let* $S_1 = (S_{\boldsymbol{p}_1,\boldsymbol{\Xi}_1})^d$ *be a d-dimensional space of vector valued splines, and* $S_2 = S_{\boldsymbol{p}_2,\boldsymbol{\Xi}_2}$ *be a space of continuous d-dimensional scalar-valued splines. Assume* (40) *and, for all* $i = 1, \dots, d$, *let* $\Xi_{2,i}$ *be an open knot vector. If*

$$\begin{cases} \forall i = 1, \dots, d, \ (23) \textit{ holds for the spaces } S_{p_{1,i},\Xi_{1,i}} \textit{ and } \partial S_{p_{2,i},\Xi_{2,i}}, \\ \forall i = 1, \dots, d, \ (23) \textit{ holds for the spaces } S_{p_{1,i},\Xi_{1,i}} \textit{ and } S_{p_{2,i},\Xi_{2,i}}, \end{cases} \tag{47}$$

then for all non-constant $g \in S_2$ *there exists* $\boldsymbol{f} \in S_1$ *such that*

$$\int_{\mathbb{R}^d} \boldsymbol{f}(\boldsymbol{x}) \cdot \nabla g(\boldsymbol{x})\, d\boldsymbol{x} \neq 0. \tag{48}$$

Proof. Recalling Remark 2.4, the implication follows immediately from Theorem 3.13, since

$$\int_{\mathbb{R}^d} \boldsymbol{f}(\boldsymbol{x}) \cdot \nabla g(\boldsymbol{x})\, d\boldsymbol{x} = \sum_{i=1}^{d} \int_{\mathbb{R}^d} f_i(\boldsymbol{x}) \frac{\partial}{\partial x_i} g(\boldsymbol{x})\, d\boldsymbol{x}.$$

□

4 Application to the Stokes problem

4.1 Setting of the problem

The usual notation of Hilbert spaces is adopted: $L^2(\Omega)$ is the space of the square integrable functions on Ω, $H^1(\Omega)$ is the subspace of $L^2(\Omega)$ of the functions whose first order partial derivatives are in $L^2(\Omega)$, $H^1_0(\Omega)$ is the subspace of $H^1(\Omega)$ of the functions with zero trace on the boundary $\partial\Omega$, $L^2_0(\Omega)$ is the subspace of $L^2(\Omega)$ of the functions with zero mean value and $H^{-1}(\Omega)$ is the dual of $H^1_0(\Omega)$.

The mathematical formulation of the Stokes problem is: find the *velocity* $\boldsymbol{u} : \mathbb{R}^d \to \mathbb{R}^d$ and *pressure* $\pi : \mathbb{R}^d \to \mathbb{R}$ such that

$$\begin{aligned} -\nu\Delta\boldsymbol{u} + \nabla\pi &= \boldsymbol{f} \quad \text{in } \Omega, \\ \nabla\cdot\boldsymbol{u} &= 0 \quad \text{in } \Omega, \\ \boldsymbol{u} &= 0 \quad \text{on } \partial\Omega, \end{aligned} \tag{49}$$

where $\boldsymbol{f} : \Omega \to \mathbb{R}^d$ is given and the viscosity parameter ν is strictly positive and assumed constant in this paper. For the sake of simplicity, we only consider homogeneous Dirichlet boundary condition in (49).

For $\boldsymbol{f} \in \left(H^{-1}(\Omega)\right)^d$, the corresponding variational form is: find $\boldsymbol{u} \in H^1_0(\Omega)^d$ and $\pi \in L^2_0(\Omega)$ such that

$$\nu\langle\nabla\boldsymbol{u},\, \nabla\boldsymbol{w}\rangle - \langle\nabla\cdot\boldsymbol{w},\, \pi\rangle = \langle\boldsymbol{f},\, \boldsymbol{w}\rangle \qquad \forall\boldsymbol{w} \in H^1_0(\Omega)^d, \tag{50a}$$

$$\langle\nabla\cdot\boldsymbol{u},\, q\rangle = 0 \qquad \forall q \in L^2(\Omega). \tag{50b}$$

The key ingredient for the stability and well-posedness of Galerkin discretizations of (50) is the *inf-sup* condition (see [8])

$$\inf_{q\in P_h} \sup_{\boldsymbol{w}\in V_h} \frac{\langle\nabla\cdot\boldsymbol{w},\, q\rangle}{\|\boldsymbol{w}\|_{H^1(\Omega)^d}\|q\|_{L^2}} \geq C_{\inf\sup}, \tag{51}$$

where $V_h \subset H^1_0(\Omega)^d$ and $P_h \subset L^2(\Omega)$ are the spaces of discrete velocities and pressures corresponding to a mesh $\mathcal{T}_h$, and $C_{\inf\sup}$ is a strictly positive constant independent of h. In this work, we will take into consideration various NURBS-based discrete spaces. Note that standard B-Spline spaces are included in the NURBS formalism.

4.2 The macroelement technique for NURBS spaces

For the proof of (51) we will make use of the so-called *macroelement* technique, developed in [23, 24] for the stability analysis of finite element discretizations based on quadratic C^0 velocities and linear C^0 pressures. When applying the macroelement technique in this context, one first make use of the so called Verfürth trick. It states that under common properties of the discrete spaces V_h and P_h defined on a mesh $\mathscr{T}_h = \{K\}$, and assuming, for the sake of simplicity, $P_h \subset H^1(\Omega)$, the $\inf\sup$ condition (51) is implied by the weaker $\inf\sup$ condition: $\exists C_{Verf} > 0$ such that

$$\inf_{q\in P_h/\mathbb{R}} \sup_{\boldsymbol{w}\in V_h} \frac{\langle\boldsymbol{w},\, \nabla q\rangle}{|\boldsymbol{w}|_{H^1(\Omega)^d}|q|_h} \geq C_{Verf}, \tag{52}$$

where $|q|_h$ is a mesh dependent norm on P_h defined by

$$|q|_h^2 = \sum_{K\in\mathscr{T}_h} h_K^2 |q|^2_{H^1(K)} \tag{53}$$

with $h_K = \mathrm{diam}(K)$.

The macroelement technique consists in reducing the global $\inf\sup$ stability condition to a local $\inf\sup$ condition for a class of sub-meshes, the macroelements. A macroelement $\mathcal{M}$ is a subset of $\mathscr{T}_h$

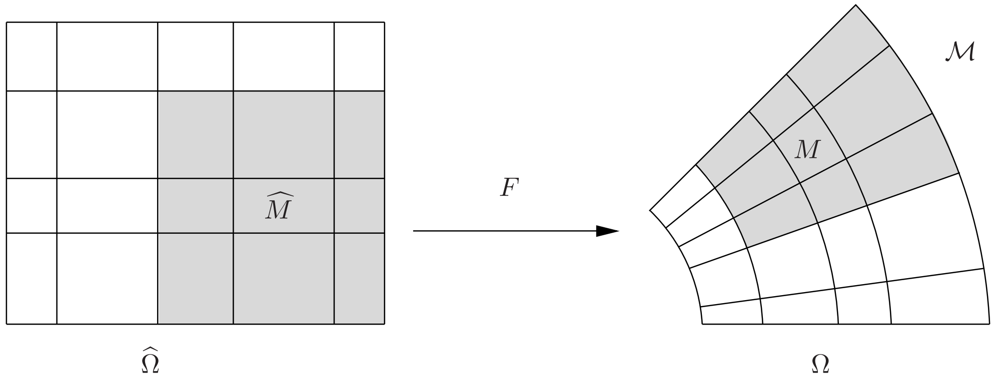

Figure 1: Examples of a 3×3 macroelement $\mathcal{M}$, its domain M is the shadowed area inside Ω on the right and the pre-image $\widehat{M} \subset \widehat{\Omega}$ of M is on the left.

such that all elements in $\mathcal{M}$ are adjacent. In our case, we will select macroelements formed by a tensor product array of elements, grouping $L \times \ldots \times L = L^d$ elements (L in each direction), as shown in Figure 1. We will select L suitably in the next Theorems 4.2–4.4. To each macroelement $\mathcal{M} \subset \mathscr{T}_h$ are associated a domain $M = \cup_{K \in \mathcal{M}} \overline{K}$ and two discrete spaces

$$V_{\mathcal{M}} = \{w \in V_h : \operatorname{supp} w \subset M\}, \tag{54}$$

$$P_{\mathcal{M}} = \{q|_M - |M|^{-1} \int_M q(X)\, dx : q \in P_h\} \tag{55}$$

Proposition 4.1 (Macroelement technique [23, 24, 7]). *If there exist constants $C_{overlap}$, C_{elem}, $C_{macro} > 0$ such that for all h it is possible to exhibit a collection of macroelements $\mathfrak{M}_h$ with the following properties*

- *$\forall K \in \mathscr{T}_h$, there exists a macroelement in $\mathfrak{M}_h$ containing K;*
- *$\forall K \in \mathscr{T}_h$, there are at most $C_{overlap}$ macroelements in $\mathfrak{M}_h$ containing K;*
- *$\forall \mathcal{M} \in \mathfrak{M}_h$, $\mathcal{M}$ contains (at most) C_{elem} elements $K \in \mathscr{T}_h$;*
- *$\forall \mathcal{M} \in \mathfrak{M}_h$,*

$$\inf_{q \in P_{\mathcal{M}}} \sup_{\boldsymbol{w} \in V_{\mathcal{M}}} \frac{\langle \boldsymbol{w}, \nabla q \rangle}{|\boldsymbol{w}|_{H^1(\Omega)^d} |q|_h} \geq C_{macro}, \tag{56}$$

  where $|q|_h^2 = \sum_{K \in \mathcal{M}} h_K^2 |q|_{H^1(K)}^2$.

then $\exists C_{Verf} > 0$ such that (52) holds.

Then, one can prove that (56) holds for suitable isogeometric spaces V_h and P_h (that is, constructed by NURBS as discussed in Section 2.2). For $\boldsymbol{w} \in V_{\mathcal{M}}$ and $q \in P_{\mathcal{M}}$ let

$$\begin{aligned} \widehat{\boldsymbol{w}} &= \boldsymbol{w} \circ F, & \widehat{q} &= q \circ F, \\ \widehat{\boldsymbol{w}}_S &= \omega(\boldsymbol{w} \circ F), & \widehat{q}_S &= \omega(q \circ F) - |\widehat{M}|^{-1} \int_{\widehat{M}} \omega(q \circ F)\, dx. \end{aligned} \tag{57}$$

The functions $\widehat{\boldsymbol{w}_S}$ and $\widehat{q}_S$ are splines on $\widehat{M} = F^{-1}(M)$, that we assume be defined on the whole $\mathbb{R}^d$, after zero extension. We define $S_{V,\mathcal{M}}$ to be the spline space spanned by $\{\widehat{\boldsymbol{w}}_S\}$, and define $S_{P,\mathcal{M}}$ as the span of $\{\widehat{q}_S\}$. ; in this way $S_{P,\mathcal{M}}$ is the intersection of a spline spaces whose function are supported in $\widehat{M} = F^{-1}(M)$ with $L_0^2(\mathbb{R}^d)$. We recall that, having adopted the isoparametric paradigm, on each macroelement the components of the the velocity field belong to the same discrete space, that is, there exists a spline space W (dependent on $\mathcal{M}$) such that $S_{V,\mathcal{M}} = W^d$. Furthermore we assume that the meshes are shape-regular, that is

$$\exists C_{shape} : \forall \mathscr{T}_h, \forall K \in \mathscr{T}_h, \quad \frac{h_K}{\rho_K} \leq C_{shape}, \tag{58}$$

where h_K is the diameter of the element K and ρ_K is the maximum diameter of a contained circle.

Under the assumptions above the inf sup condition (56) can be reduced to the condition

$$\forall \widehat{q}_S \in S_{P,\mathcal{M}},\, \exists \widehat{\boldsymbol{w}}_S \in S_{V,\mathcal{M}} \, : \, \int_{\mathbb{R}^d} \widehat{\boldsymbol{w}}_S(\boldsymbol{x}) \cdot \nabla \widehat{q}_S(\boldsymbol{x}) \, d\boldsymbol{x} \neq 0. \tag{59}$$

Indeed by (59) it follows that $\forall \mathcal{M} \in \mathfrak{M}_h$ there exists $C_S(\mathcal{M}) > 0$ such that

$$\inf_{q \in P_{\mathcal{M}}} \sup_{\boldsymbol{w} \in V_{\mathcal{M}}} \frac{\langle \widehat{\boldsymbol{w}}_S,\, \nabla \widehat{q}_S \rangle}{|\widehat{\boldsymbol{w}}_S|_{H^1(\widehat{\Omega})^d} |\widehat{q}_S|_h} \geq C_S(\mathcal{M}), \tag{60}$$

where $|\cdot|_h^2 = \sum_{K \in \mathcal{M}} h_K^2 |\cdot|^2_{H^1(\widehat{K})}$, with $K = F(\widehat{K})$, is a norm on the space $S_{P,\mathcal{M}}$, since the null-average property. A positive lower bound on $C_S(\mathcal{M})$ is obtained by the following compactness argument. Let Ψ be the inclusion of the macroelements in the unit sphere of $\mathbb{R}^{dL}$ obtained by using the lengths of their edges as coordinates and then normalizing (recall that we are considering macroelements made of L^d elements, see Figure 1). The function $C_S(\mathcal{M})$ is scaling invariant and thus can be factorized as $C_S = \widehat{C}_S \circ \Psi$. From the regularity conditions (58) it follows that the image of the macroelements of interest in the sphere of $\mathbb{R}^{dL}$ is in fact included in a compact set, where $\widehat{C}_S$ is well defined, continuous, and strictly positive. This implies the existence of a constant $C_S > 0$ such that for all $\mathcal{M} \in \mathfrak{M}_h$, $C_S(\mathcal{M}) \geq C_S$.

From (60), by using norm equivalences and approximating the weight ω by a macroelement-wise constant it follows that $\exists \tilde{h}, \exists C_N > 0$ such that $\forall h < \tilde{h}$, $\forall \mathcal{M} \in \mathfrak{M}_h$

$$\inf_{q \in P_{\mathcal{M}}} \sup_{\boldsymbol{w} \in V_{\mathcal{M}}} \frac{\langle \widehat{\boldsymbol{w}},\, \nabla \widehat{q} \rangle}{|\widehat{\boldsymbol{w}}|_{H^1(\widehat{\Omega})^d} |\widehat{q}|_h} \geq C_N. \tag{61}$$

Furthermore, approximating F by a linear map on each macroelement (F is piecewise C^∞) and using again norm equivalences it follows that $\exists \bar{h}, \exists C_{Verf} > 0 : \forall h < \bar{h}$, $\forall \mathcal{M} \in \mathfrak{M}_h$

$$\inf_{q \in P_{\mathcal{M}}} \sup_{\boldsymbol{w} \in V_{\mathcal{M}}} \frac{\langle \boldsymbol{w},\, \nabla q \rangle}{|\boldsymbol{w}|_{H^1(\Omega)^d} |q|_h} \geq C_{macro}. \tag{62}$$

In conclusion, for any NURBS space pair satisfying the assumptions above and (59) the inf sup stability condition holds, at least for $h < \bar{h}$. More details of this construction can be found in [7].

4.3 Examples of inf sup stable NURBS spaces

Two families of NURBS space pairs that fulfill (59) are presented in this section. The first family is an extension of the classical Taylor-Hood finite element, and has been already tested in [4, 9] and studied in [4, 7] for C^0 and C^1 regularity. It is originated by $(p+1)$-degree velocities and p-degree pressures defined on the same mesh, typically with the same global regularity. We refer to this family by *isogeometric TH element*. For the second family the velocity field is defined on a *subgrid* of the pressure grid, e.g., by subdividing each pressure element into 2^d velocity elements. This construction allows us to take both fields as NURBS with highest smoothness, for example $(p+1)$-degree C^p continuous velocities and p-degree C^{p-1} continuous pressures. This family is referred as *isogeometric SG element*.

We adopt the notation and assumptions of Section 2.2. In particular, the geometrical map is $F \in N_{p_0,r_0,\boldsymbol{\mathcal{Z}}_0}$ and all the NURBS spaces introduced in Theorem 4.2 and 4.4 are refinement of $N_{p_0,r_0,\boldsymbol{\mathcal{Z}}_0}$.

Theorem 4.2 (Isogeometric *TH* element)**.** *Let $p_V, r_V, p_P, r_P \in \mathbb{R}$ such that*

$$\begin{cases} p_V > r_V \geq 0 \\ p_P > r_P \geq 0 \\ p_V - r_V > p_P - r_P; \end{cases} \tag{63}$$

then there exists $\bar{h} = \bar{h}(\Omega, C_{shape}, p_V, r_V, p_P, r_P)$ such that the TH pair

$$V_{p_V,r_V,h} = \left\{ f \circ F^{-1} : f \in (N_{p_V,r_V,h})^d \right\}, \tag{64}$$

$$P_{p_P,r_P,h} = \left\{ g \circ F^{-1} : g \in N_{p_P,r_P,h} \right\}, \tag{65}$$

satisfies the inf sup *condition (51) for all $h \leq \bar{h}$.*

Proof. By the results summarized in Section 4.2, it is sufficient to exhibit a family of macroelements $\mathfrak{M}_h$ such that (59) holds. We will select macroelements made by L^d elements. To each macroelement $\mathcal{M} \in \mathfrak{M}_h$ is associated the vector of knot vectors (without repetitions) $\boldsymbol{\mathcal{Z}}_{\mathcal{M}} = (\mathcal{Z}_{1,\mathcal{M}}, \ldots, \mathcal{Z}_{d,\mathcal{M}})$ where

$$\begin{aligned} \mathcal{Z}_{1,\mathcal{M}} &= (\zeta_{1,i_1}, \ldots, \zeta_{1,i_1+L}) \\ &\vdots \\ \mathcal{Z}_{d,\mathcal{M}} &= (\zeta_{d,i_d}, \ldots, \zeta_{d,i_d+L}), \end{aligned}$$

such that $\widehat{M} = [\zeta_{1,i_1}, \zeta_{1,i_1+L}] \times \ldots \times [\zeta_{d,i_d}, \zeta_{d,i_d+L}]$. Then, the spaces $S_{V,\mathcal{M}}$ and $S_{P,\mathcal{M}}$ that appear in (59) can be written as

$$\begin{aligned} S_{V,\mathcal{M}} &= (\mathring{S}_{p_V,r_V,\boldsymbol{\mathcal{Z}}_{\mathcal{M}}})^d, \\ S_{P,\mathcal{M}} &= S_{p_P,r_P,\boldsymbol{\mathcal{Z}}_{\mathcal{M}}} \cap L^2_0. \end{aligned}$$

Recalling Corollary 3.14, it is sufficient to show that condition (23) holds, in each tensor component i, for the pairs of spaces S_1, S_2 with

$$S_1 = \mathring{S}_{p_V,r_V,\mathcal{Z}_{i,\mathcal{M}}}, \quad S_2 = S_{p_P,r_P,\mathcal{Z}_{i,\mathcal{M}}},$$

and

$$S_1 = \mathring{S}_{p_V,r_V,\mathcal{Z}_{i,\mathcal{M}}}, \quad S_2 = \partial S_{p_P,r_P,\mathcal{Z}_{i,\mathcal{M}}} = S_{p_P-1,r_P-1,\mathcal{Z}_{i,\mathcal{M}}}.$$

All the pairs above have already been considered in Proposition 3.11, and since (63) we only have to require $\dim S_2 \leq \dim S_1$. It is easy to check that the last condition holds in both cases selecting $L \geq \frac{r_V+r_P+2}{(p_V-r_V)-(p_P-r_P)}$ (notice that $L \geq p_V + p_P$ suffices).

It is clear that we can easily define $\mathcal{M}_h$ such that the macroelements, as described above, cover the whole domain, and, taking h small enough, the map F is C^∞ on each $\widehat{M}$. □

Remark 4.3. In particular the pair $V_{p+1,r,h}$ and $P_{p,r,h}$ is inf sup stable for any $0 \leq r \leq p-1$. This is the most interesting choice because it balances the error in the velocity and pressure terms and will be tested in Section 5.

To introduce the *SG* family of elements, we consider the mesh $\mathscr{T}_h$ and its refinement $\mathscr{T}_{h/2}$, which is obtained subdividing each element $K \in \mathscr{T}_h$ into 2^d elements in a uniform way.

Then we have the following result.

Theorem 4.4 (Isogeometric *SG* element)**.** *Let $p_V, r_V, p_P, r_P \in \mathbb{R}$ such that*

$$\begin{cases} p_V > r_V \geq 0 \\ p_P > r_P \geq 0 \\ 2(p_V - r_V) > p_P - r_P, \end{cases} \tag{66}$$

then there exists $\bar{h} = \bar{h}(\Omega, C_{shape}, p_V, r_V, p_P, r_P)$ *such that the SG pair*

$$V_{p_V,r_V,h/2} = \left\{ f \circ F^{-1} : f \in (N_{p_V,r_V,h/2})^d \right\}, \tag{67}$$

$$P_{p_P,r_P,h} = \left\{ g \circ F^{-1} : g \in N_{p_P,r_P,h} \right\}; \tag{68}$$

satisfies the inf sup *condition (51) for all* $h \leq \bar{h}$*.*

Proof. The proof is in fact analogous to the one of Theorem 4.2, with the difference that Proposition 3.12 is used now instead of Proposition 3.11. The details are omitted. ☐

Remark 4.5. Now the *SG* pair $V_{p+1,p,h/2}$ and $P_{p,p-1,h}$ is the most interesting one, since it is inf sup stable, it uses NURBS functions with maximal regularity for both spaces, and velocity-pressure errors are balanced. This will be tested in Section 5.

Remark 4.6. Using the same kind of macroelements as in the Theorems 4.2–4.4 one can derive sufficient conditions for the stability of a wider class of methods. For instance it is possible to insert low regularity interfaces in the domain as long as they are at least one macroelement apart, such that it is still possible to cover the domain by macroelements. This will be tested in Section 5. Furthermore, macroelements with variable internal regularity can be built and studied from the general result of Theorem 3.10.

5 Numerical testing

In this section we perform numerical testing of the isogeometric elements introduced and studied in Section 4.3.

5.1 Two-dimensional benchmarks

In the first test problem we aim to confirm numerically and compare the accuracy of the proposed *TH* and *SG* isogeometric elements. We solve the Stokes problem (49) with homogeneous Dirichlet boundary condition on the quarter of annulus (see Figure 2). The coarse mesh is made by a single element where the NURBS parametrization F is C^∞. The forcing term $\boldsymbol{f}$ is set in order to have exact solution

$$\boldsymbol{u} = \begin{pmatrix} 2y(x-y)(x^2+y^2-4)(x^2+y^2-1) \\ (x^5 - 2x^4y + 6x^3y^2 - 5x^3 - 8x^2y^3 + 10x^2y \\ +5xy^4 - 15xy^2 + 4x - 6y^5 + 20y^3 - 8y) \\ \\ -2y^2(x-y)(x^2+y^2-4)(x^2+y^2-1) \\ (5x^4 - 4x^3y + 6x^2y^2 - 15x^2 \\ -4xy^3 + 10xy + y^4 - 5y^2 + 4) \end{pmatrix}, \tag{69}$$

$$\pi = e^{\frac{y}{x}} - e^{\frac{x-y}{x+y}}. \tag{70}$$

In Figure 3 we show the numerical errors $\|\boldsymbol{u} - \boldsymbol{u}_h\|_{H^1_0(\Omega)}$ and $\|\pi - \pi_h\|_{L^2(\Omega)}$ versus the total number of degrees of freedom n_{dof}, for the isogeometric *TH* pair $V_{p+1,r,h}$ and $P_{p,r,h}$. Uniform refinement in radial and angular direction is performed. It is seen that the tested *TH* elements deliver the expected order of approximation, that is, $n_{dof}^{(p+1)/2}$. We compare the two cases $r = 0$ and $r = p-1$ and observe that, as expected, the smooth approximation delivers a more accurate solution when n_{dof} is the same.

In Figure 4, we repeat the same tests for the isogeometric *SG* elements $V_{p+1,p,h/2}$ and $P_{p,p-1,h}$, only considering the smoothest approximation. Observe the optimal error decay in all cases, the

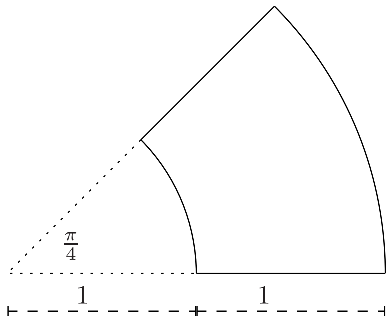

Figure 2: Two-dimensional domain for the benchmarks of Section 5.1

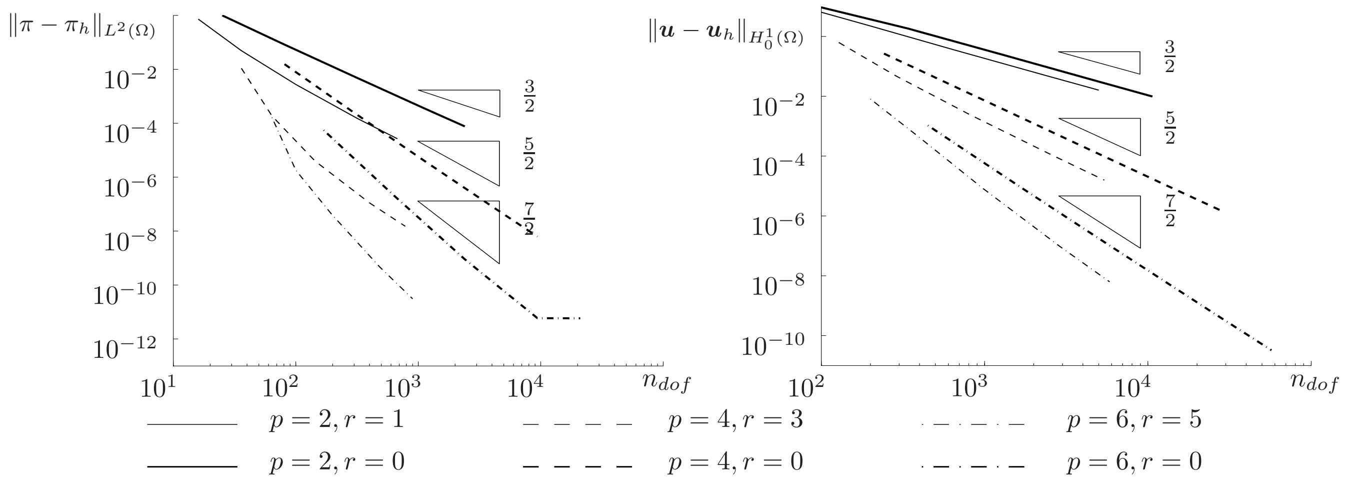

Figure 3: Error plots for the isogeometric *TH* element $V_{p+1,r,h}$ and $P_{p,r,h}$ in the two-dimensional benchmark.

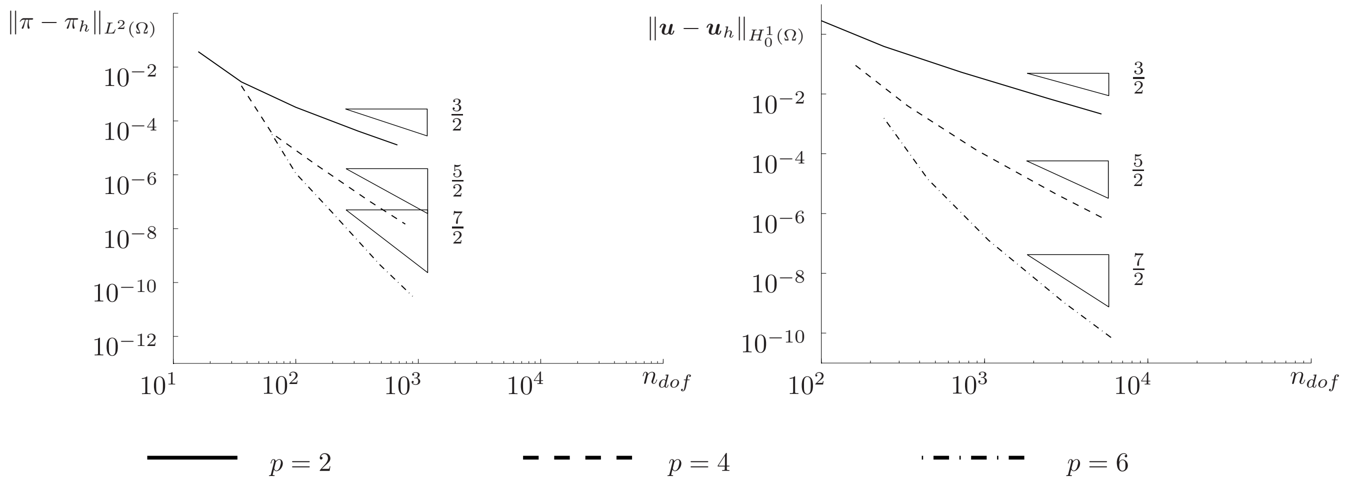

Figure 4: Error plots for the isogeometric *SG* element $V_{p+1,p,h/2}$ and $P_{p,p-1,h}$.

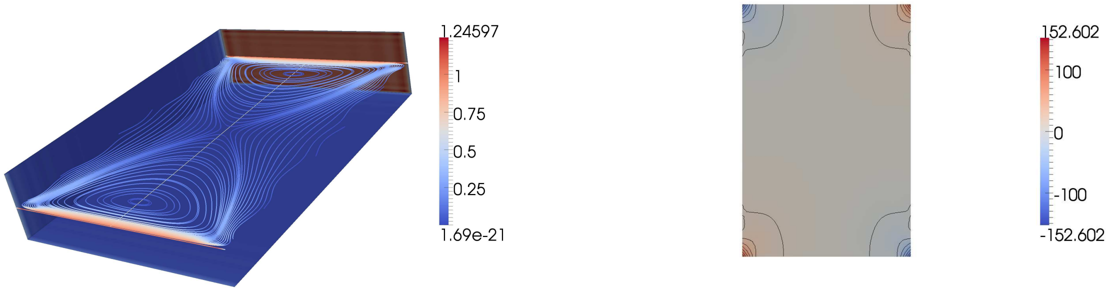

Figure 5: Driven cavity. On the left, velocity streamlines on the midsurface $z = 0.15$. On the right, pressure on the same midsurface, with 20 contour levels between -150 and 150.

isogeometric *SG* velocity approximation being more accurate, given n_{dof}, than the isogeometric *TH* approximation. This is consistent with the known result that smoothest spline or NURBS give the highest accuracy per degree-of-freedom when approximating smooth functions (see [15]).

5.2 Three-dimensional benchmark

We consider now two different benchmark with the aim of studying the numerical stability of the new *SG* element.

The first problem is the Stokes flow in a driven cavity. The domain is the cuboid $[0, 1] \times [0, 1.5] \times [0, 0.3]$. Homogeneous Dirichlet boundary condition is imposed on the lateral boundary, while on the other two faces $y = 0$ and $y = 1.5$ the velocity is set to $(-1, 0, 0)$ and $(1, 0, 0)$, respectively. The discrete solution is obtained by a *SG* element on a $8 \times 8 \times 8$ grid for the pressure, $16 \times 16 \times 16$, for the velocity. The pressure degree and regularity are $p_P = 2$ and $r_P = 1$, while for the velocity unknown we select $p_V = 3$ and $r_V = 2$. The total number of degrees of freedom is 15738 (14739 for the velocity and 999 for the pressure). The result of this simulation is depicted in Figure 5. It is observed, in particular, that the pressure field is stable and correctly approximates the singularities at the four edges where the boundary datum is discontinuous.

In the second test problem we simulate the Stokes flow in a three-dimensional pipe. The pipe inlet is the rectangle $[-0.5, 0.5] \times [-0.25, 0.25]$ in the plane $x = -2$. The rectangular cross section is twisted in the central part $x \in [-1, 1]$ by $\frac{\pi}{2}$, see Figure 6 (left). The problem is designed in order to test the case of a geometry parametrization which is only C^0 at some interfaces: this happens between the first and the middle twisted part (at $x = -1$) and between the twisted and last part of the pipe (at $x = 1$). Our macroelement stability analysis covers this case (see Remark 4.6). The fluid is drawn by a unitary surface load at the ends of the pipe and homogeneous Dirichlet boundary condition is imposed on the lateral surface of the pipe. We test the the *SG* element on a $18 \times 6 \times 6$ grid for the pressure, $36 \times 12 \times 12$ subgrid for the velocity field. The pressure degree and regularity are $p_P = 3$ and $r_P = 2$, the velocity degree and regularity are $p_V = 4$ and $r_V = 3$. The total number of degrees of freedom is 29073 (27048 for the velocity and 2025 for the pressure). The results of this simulation are shown in Figure 6, 7.

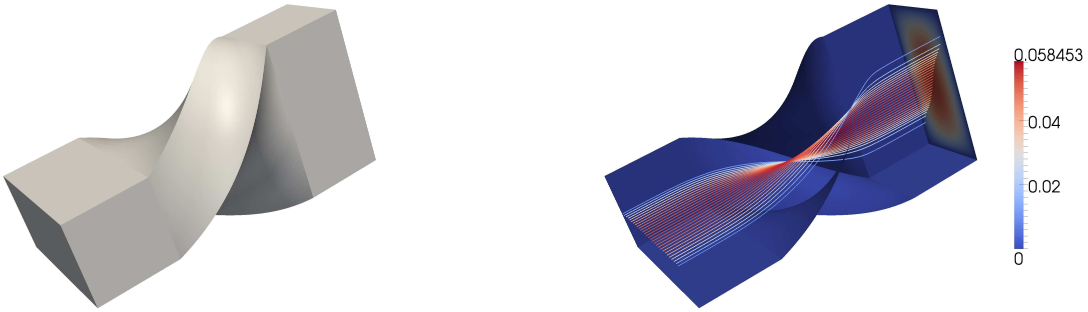

Figure 6: Twisted pipe. On the left, the domain. On the right, velocity streamlines originated from the inlet midline $x = -2, y \in [-.5, .5], z = 0$.

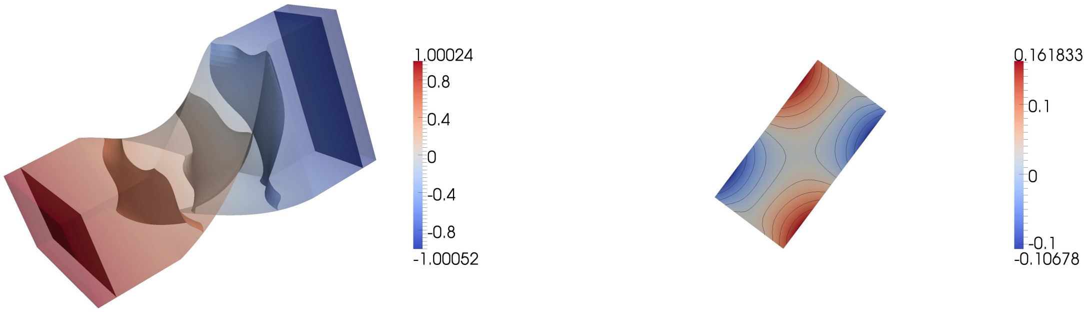

Figure 7: Twisted pipe. On the left, 5 contour surfaces of the pressure between -0.9 and 0.9. On the right, 10 pressure contour lines betwen -0.1 and 0.16 on the midsection $x = 0$.

Acknowledgments

The authors were partially supported by the European Research Council through the FP7 Ideas Starting Grant 205004 *GeoPDEs - Innovative compatible discretization techniques for partial differential equations*, and by the Italian MIUR through the FIRB "Futuro in Ricerca" Grant RBFR08CZ0S *Discretizzazioni Isogeometriche per la Meccanica del Continuo*. Giancarlo Sangalli was also partially supported by the European Research Council Ideas Starting Grant 259229 *ISOBIO - Isogeometric Methods for Biomechanics*. This support is gratefully acknowledged.

References

[1] F. Auricchio, L. Beirão da Veiga, A. Buffa, C. Lovadina, A. Reali, and G. Sangalli, *A fully "locking-free" isogeometric approach for plane linear elasticity problems: a stream function formulation.*, Comput. Methods Appl. Mech. Eng., 197 (2007), pp. 160–172.

[2] Y. Bazilevs, V. Calo, J. Cottrell, T. Hughes, A. Reali, and G. Scovazzi, *Variational multiscale residual-based turbulence modeling for large eddy simulation of incompressible flows.*, Comput. Methods Appl. Mech. Eng., 197 (2007), pp. 173–201.

[3] Y. Bazilevs, V. Calo, T. Hughes, and Y. Zhang, *Isogeometric fluid-structure interaction: Theory, algorithms, and computations.*, Comput. Mech., 43 (2008), pp. 3–37.

[4] Y. Bazilevs, L. a. Da Veiga, J. Cottrell, T. Hughes, and G. Sangalli, *Isogeometric analysis: Approximation, stability and error estimates for h-refined meshes.*, Math. Models Methods Appl. Sci., 16 (2006), pp. 1031–1090.

[5] Y. Bazilevs, C. Michler, V. Calo, and T. Hughes, *Isogeometric variational multiscale modeling of wall-bounded turbulent flows with weakly enforced boundary conditions on unstretched meshes.*, Comput. Methods Appl. Mech. Eng., 199 (2010), pp. 780–790.

[6] L. Beirão da Veiga, A. Buffa, J. Rivas, and G. Sangalli, *Some estimates for h-p-k-refinement in isogeometric analysis.*, Numer. Math., 118 (2011), pp. 271–305.

[7] A. Bressan, *"isogeometric regular discretization for the stokes problem"*, IMA Journal of Numerical Analysis, (2010).

[8] F. Brezzi and M. Fortin, *Mixed and hybrid finite element methods.*, Springer Series in Computational Mathematics. 15. New York etc.: Springer-Verlag. ix, 350 p. , 1991.

[9] A. Buffa, C. de Falco, and G. Sangalli, *Isogeometric analysis: stable elements for the 2d stokes equation*, International Journal for Numerical Methods in Fluids, 65 (2011), pp. 1407–1422.

[10] A. Buffa, J. Rivas, G. Sangalli, and R. Vázquez, *Isogeometric discrete differential forms in three dimensions*, SIAM Journal on Numerical Analysis, 49 (2011), p. 818.

[11] A. Buffa, G. Sangalli, and R. Vázquez, *Isogeometric analysis in electromagnetics: B-splines approximation*, Computer Methods in Applied Mechanics and Engineering, 199 (2010), pp. 1143–1152.

[12] J. Cottrell, T. Hughes, and Y. Bazilevs, *Isogeometric analysis: toward integration of CAD and FEA*, John Wiley & Sons Inc, 2009.

[13] J. Cottrell, A. Reali, Y. Bazilevs, and T. Hughes, *Isogeometric analysis of structural vibrations.*, Comput. Methods Appl. Mech. Eng., 195 (2006), pp. 5257–5296.

[14] C. De Boor, *A practical guide to splines*, vol. 27, Springer Verlag, 2001.

[15] J. Evans, Y. Bazilevs, I. Babuska, and T. Hughes, *N-widths, sup-infs, and optimality ratios for the k-version of the isogeometric finite element method*, Computer Methods in Applied Mechanics and Engineering, 198 (2009), pp. 1726–1741.

[16] H. Gomez, T. Hughes, X. Nogueira, and V. Calo, *Isogeometric analysis of the isothermal navier-stokes-korteweg equations*, Computer Methods in Applied Mechanics and Engineering, 199 (2010), pp. 1828–1840.

[17] T. Goodman, *New bounds on the zeros of spline functions.*, J. Approximation Theory, 76 (1994), pp. 123–130.

[18] T. Hughes, J. Cottrell, and Y. Bazilevs, *Isogeometric analysis: Cad, finite elements, nurbs, exact geometry and mesh refinement*, Computer methods in applied mechanics and engineering, 194 (2005), pp. 4135–4195.

[19] T. Hughes, A. Reali, and G. Sangalli, *Duality and unified analysis of discrete approximations in structural dynamics and wave propagation: comparison of p-method finite elements with k-method nurbs*, Computer methods in applied mechanics and engineering, 197 (2008), pp. 4104–4124.

[20] S. Lipton, J. Evans, Y. Bazilevs, T. Elguedj, and T. Hughes, *Robustness of isogeometric structural discretizations under severe mesh distortion*, Computer Methods in Applied Mechanics and Engineering, 199 (2010), pp. 357–373.

[21] L. Piegl and W. Tiller, *The NURBS book*, Springer Verlag, 1997.

[22] L. Schumaker, *Spline functions: basic theory*, Krieger (Malabar, Fla.), 1993.

[23] R. Stenberg, *Analysis of mixed finite element methods for the Stokes problem: A unified approach.*, Math. Comput., 42 (1984), pp. 9–23.

[24] ———, *Error analysis of some finite element methods for the Stokes problem.*, Math. Comput., 54 (1990), pp. 495–508.

[25] C. Taylor and P. Hood, *A numerical solution of the navier-stokes equations using the finite element technique*, Computers & Fluids, 1 (1973), pp. 73–100.